JOURNAL OF AIRCRAFT
Vol. 31, No. 5, Sept.–Oct. 1994

Application of Circulation Control to Advanced Subsonic Transport Aircraft, Part I: Airfoil Development

Robert J. Englar,* Marilyn J. Smith,† Sean M. Kelley,‡ and Richard C. Rover III‡
Georgia Tech Research Institute, Atlanta, Georgia 30332

An experimental/analytical research program was undertaken to develop advanced versions of circulation control wing (CCW) blown high-lift airfoils, and to address specific issues related to their application to subsonic transport aircraft. The primary goal was to determine the feasibility and potential of these pneumatic airfoils to increase high-lift system performance in the terminal area while reducing system complexity. A four-phase program was completed, including 1) experimental development and evaluation of advanced CCW high-lift configurations, 2) development of effective pneumatic leading-edge devices, 3) computational evaluation of CCW airfoil designs plus high-lift and cruise capabilities, and 4) investigation of the terminal-area performance of transport aircraft employing these airfoils. The first three phases of this program are described in Part I of this article. Applications to the high-lift and control systems of advanced subsonic transport aircraft and resulting performance are discussed in the continuation of this article, Part II. Experimental lift coefficient values approaching 8.0 at zero incidence and low blowing rates were demonstrated by two-dimensional CCW configurations that promised minimal degradation of the airfoil's performance during cruise. These results and experimental/CFD methods will be presented in greater detail in the following discussions.

Nomenclature

C_d = airfoil drag coefficient
C_l = airfoil lift coefficient
C_μ = two-dimensional jet momentum (blowing) coefficient, trailing-edge slot
$C_{\mu\,\mathrm{LE}}$ = two-dimensional jet momentum (blowing) coefficient, leading-edge slot
c = airfoil chord length
c_f = flap chord length
h = blowing slot height, trailing edge
h_{LE} = blowing slot height, leading edge
$\dot{m}$ = jet mass flow rate per unit slot span
q = freestream dynamic pressure
r_1 = CCW flap radius of rotation
r_2 = CCW flap upper-surface radius
V_j = isentropic jet velocity
x_{slot} = longitudinal location of blowing slot
α = angle of attack
δ_f = flap deflection angle

Introduction

BASED on existing data,[1] pneumatic high-lift airfoils appear to offer significant payoffs in the design and development of next-generation subsonic transport aircraft. Both ground and flight experimental investigations have shown that a specific type of blown airfoil known as the circulation control wing (CCW) can greatly augment the high-lift capabilities of conventional mechanical flaps. Reference 1 provides summaries of some of these developments and includes verification of CCW airfoil sections generating very high lift at low blowing rates. It also discusses successful CCW applications to and flight tests on fixed-wing short takeoff and landing (STOL) and rotary-wing vertical takeoff and landing (VTOL) aircraft. The CCW concept employs tangential blowing over round or near-round trailing edges, as demonstrated on the airfoil seen in Fig. 1. Here, the lack of a sharp trailing edge avoids the Kutta condition requirement that the stagnation streamline depart the airfoil at the trailing edge. As can be seen in numerous experimental results,[2–5] the blowing jet causes the aft stagnation point to move nearly 180 deg around the round trailing edge. This action does, in fact, produce a pneumatic cambering device. The result is very high-lift generation, with two-dimensional lift coefficients greater than 7.0 being generated at 0-deg angle of attack.[2] Lift augmentation ($\Delta C_l/C_\mu$) as high as 80 or more has been reported in Refs. 1 and 6. The driving parameter is the momentum coefficient, defined for two-dimensional airfoils as

$$C_\mu = \dot{m}V_j/qc$$

Conversely, as Fig. 2 shows, a desired large lift increment due to blowing can be generated either at much lower blowing requirements than a conventional blown flap, or with a much smaller trailing-edge flap size.

In addition, high-lift system complexity can be reduced by substituting simplified pneumatic components for mechanical flaps, tracks, and actuators. Figure 1 shows a no-moving-parts CCW trailing edge applied to a NASA supercritical airfoil section.[7,8] Not only are the conventional leading-edge and trailing-edge components eliminated, but the resulting lift values (at zero incidence and up through maximum C_l) are quite significant. As this figure shows, CCW configurations applicable to transports typically generated C_l values up to 6 or 7, equal to or exceeding the high-lift potential of even the most complex multielement mechanical flap airfoils. In this case, the very large leading-edge radius of the thick blown airfoil produced attached flow up through 10-deg incidence, but it is obvious that more effective separation prevention was needed at higher incidence or higher lift. Pneumatic concepts can further simplify transport aircraft wings by eliminating the need for mechanical leading-edge devices as well as mechanical-roll-control or direct-lift-control surfaces.[9]

While the high-lift and simplifying capabilities of these CCW devices have been confirmed in experimental programs and in actual flight demonstrations on military aircraft,[10,11] specific

Presented as Paper 93-0644 at the AIAA 31st Aerospace Sciences Meeting and Exhibit, Reno, NV, Jan. 11–14, 1993; received April 27, 1993; revision received Feb. 25, 1994; accepted for publication March 7, 1994.

*Senior Research Engineer, Aerospace Sciences Laboratory. Associate Fellow AIAA.
†Senior Research Engineer, Aerospace Sciences Laboratory. Senior Member AIAA.
‡Cooperative Student, Aerospace Sciences Laboratory.

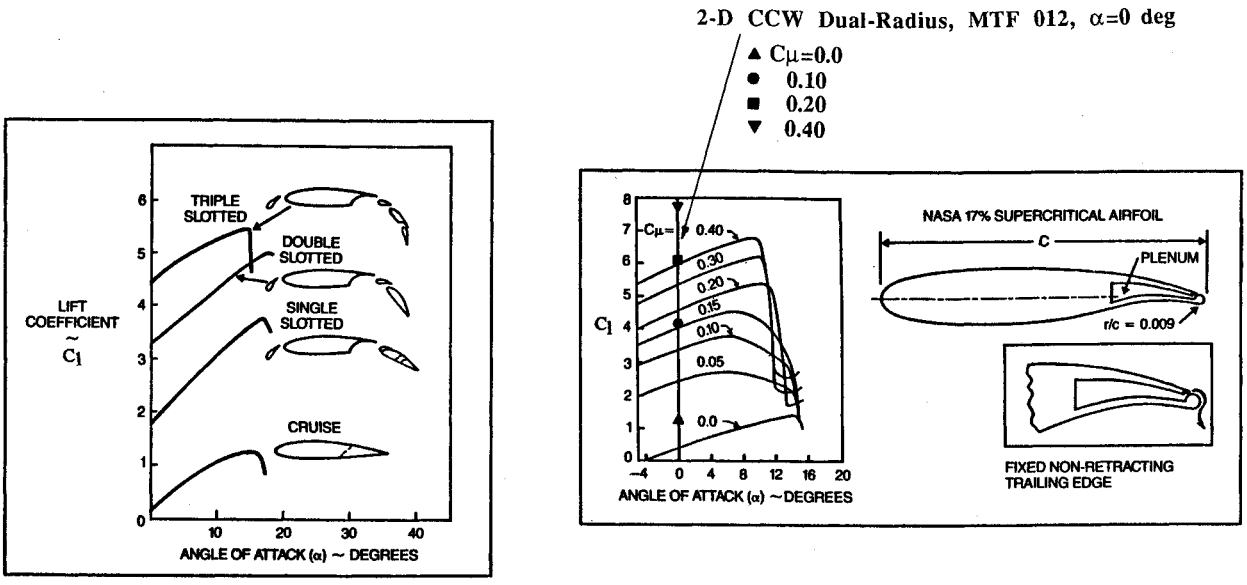

Fig. 1 Comparison of blown CCW and mechanical high-lift systems.

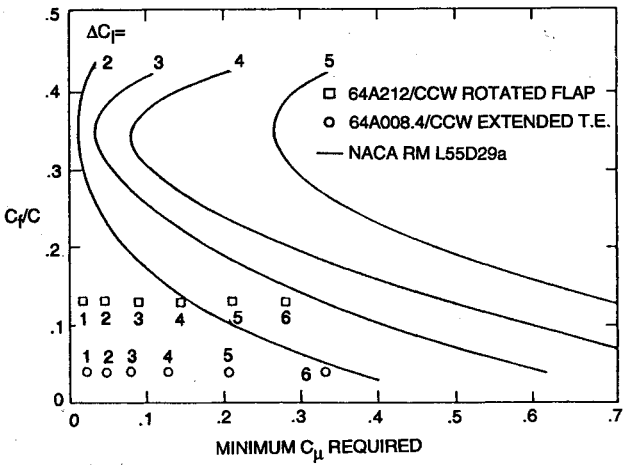

Fig. 2 Comparison of the lift-augmenting capabilities of blown flap and CCW airfoils at $\alpha = 0$ deg.

application-related issues need to be addressed to take advantage of these pneumatic benefits for transport aircraft. Research personnel at the Aerospace Sciences Laboratory of Georgia Tech Research Institute (GTRI) have been involved with experimental development and computational analysis of these circulation control concepts since their initiation in the late 1960s. The present research project was undertaken by GTRI to resolve these issues in order to make pneumatic airfoil technology available for use in next-generation transports or as retrofits on existing aircraft. Specific issues to be addressed include the development of advanced CCW airfoils while minimizing airflow and blowing requirements; determining the feasibility and efficiency of pneumatic leading-edge devices; employing CFD computational methods to guide the design of CCW systems; and finally, investigating system performance for a postulated CCW subsonic transport (see Part II of this article). Results of the two-dimensional airfoil investigations will be presented in the following sections.

Development of Advanced CCW Airfoils

Prior CCW Configurations

Previous development of CCW high-lift airfoils has yielded a number of configurations intended for both fixed-wing STOL and rotary-wing VTOL aircraft; many of these have generated high-lift augmentation at low blowing rates. Whereas this lift augmentation is significant, the drag associated with large unblown radii can be prohibitive in cruise. An attempt to reduce that drag penalty was successful,[7,8] as much smaller trailing-edge radii were incorporated into the patented bluff trailing-edge configuration on a 17% supercritical airfoil (Fig. 1). While the drag was greatly reduced, it was found that small CCW radii with larger slot heights could cause jet detachment and sudden lift loss at higher C_μ. As a compromise to the above, the dual-radius CCW configuration was developed.[8] Figure 3 shows a typical CCW configuration of this type applied to a 16% thick supercritical airfoil. This configuration improves upon the round bluff CCW in three ways. First, the short-chord flap has a sharp trailing edge in the retracted configuration, so that in cruise there is very little increase in base drag or separated flow caused by the unblown round surface. Secondly, when this short flap is deflected about an initial radius r_1, the upper surface of the flap is a uniform circular arc with larger radius r_2. This is much more conducive to increased jet turning. Thirdly, the simple mechanical deflection also provides unblown camber, which adds to the total lift capability and provides some aerodynamic lift should a blowing loss occur. These advantages offer significant gains over the fixed round CCW configurations, even at the risk of adding some mechanical complexity. Thus, the development of advanced CCW configurations under the current effort has concentrated on the evaluation of these dual-radius configurations.

Two-Dimensional Airfoil Experimental Test Setup

Accurate two-dimensional experimental evaluation of blown high-lift airfoils is not a trivial undertaking, and considerable care must be expended to perform this effort properly.[12] The primary problem that must be overcome is the interaction between the momentum deficits in the tunnel-wall boundary layers and the severe adverse pressure gradients on the blown airfoil downstream of both the leading-edge and trailing-edge flaps or blowing slots. If left uncorrected, this yields strong vorticity at these junctions and nonuniform downwash all along the airfoil span; non-two-dimensional results are guaranteed, and the true angle of attack is far less than the nominal geometric value. For the present investigations conducted in the GTRI Model Test Facility (MTF) 30- × 43-in. subsonic research tunnel, a tangential wall blowing system previously developed at GTRI to improve ground-effect investigations[13] was modified to provide combined floor and ceiling blowing

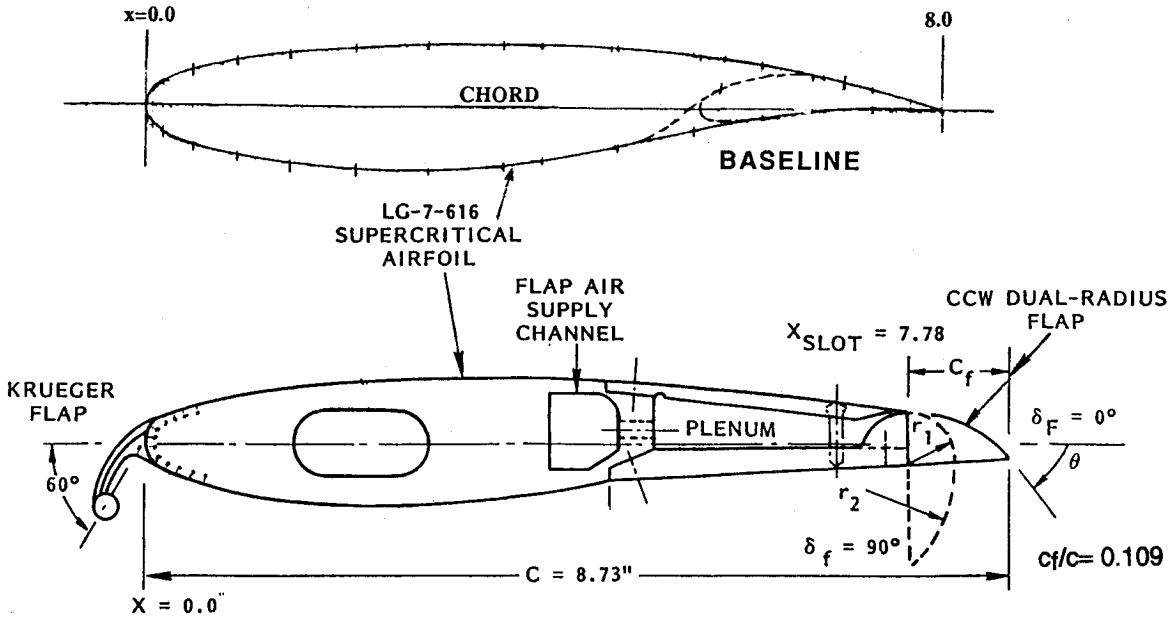

Fig. 3 Advanced dual-radius CCW configuration applied to a 16% thick supercritical two-dimensional airfoil model.

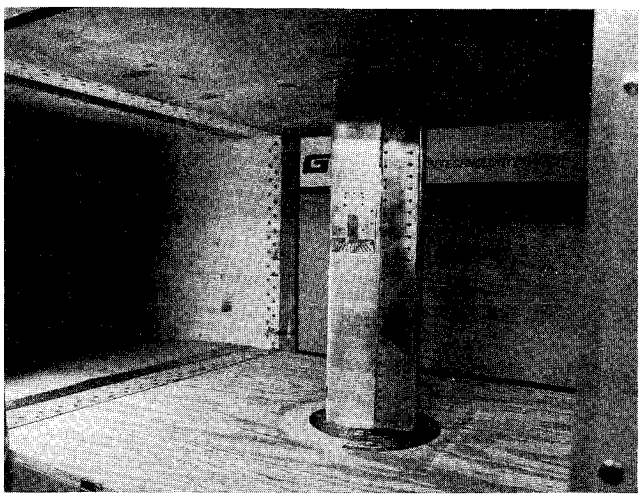

Fig. 4 Baseline two-dimensional CCW dual-radius airfoil in MTF test section, showing floor and ceiling wall blowing slots in entrance.

(Fig. 4). When applied to the present vertically-mounted airfoil tests, the calibrated wall blowing value that removed the wall interference also reduced the measured drag by up to 45% for the blown airfoils. This resulted from elimination of the induced drag due to vorticity at the walls. Static pressures measured along the model span also confirmed this blowing value as returning the spanwise flow to a near-uniform value from floor to ceiling. In addition to these spanwise pressures, chordwise static pressure measurements were taken on the model surface at midspan for comparison to CFD analytical results. Force and moment coefficients were recorded by a floor balance. The CCW model spanned almost 30 in. from tunnel floor to within $\frac{1}{16}$ in. of the tunnel ceiling, and was mounted on a 12-in.-diam base plate attached to the floor balance system. A thin endplate separated the ceiling end of the model from the wall, allowing only enough space to prevent model grounding. After the calibration of the ceiling blowing system, drag tares were taken on the base plate with wall blowing activated, and a blown tare as a function of dynamic pressure was determined. This increment was subtracted from all floor-balance data. Further explanation of test techniques, including mass flow/jet velocity tradeoffs (i.e., slot height vs pressure ratio), are given in Refs. 2, 4, 7, 8, and 12.

The airfoil of Fig. 3 was evaluated in this facility using these special two-dimensional test techniques. This configuration had previously been evaluated in the MTF tunnel as part of a powered-lift STOL program.[14] Those tests were conducted using a semi-span three-dimensional model with a constant-chord wing having this same airfoil section, and extending 26 in. from the tunnel floor, yielding an aspect-ratio-5.5 configuration. These semispan tests provided a good basis for evaluating the parameters of flap deflection, momentum coefficient, slot height and CCW turning radius, but their strong three dimensionality made them incompatible with previous high-quality two-dimensional data for other blown and mechanical-flap airfoils. Therefore, a rigorous effort was undertaken as part of the present program to accurately re-evaluate this baseline CCW dual-radius configuration as a two-dimensional airfoil. Although an improved version of this airfoil was designed using in-house CFD codes, the model conversion was not completed in time. Thus, the original dual-radius CCW/supercritical configuration of Fig. 3 was reinstalled in the GTRI Model Test Facility tunnel as a baseline reference two-dimensional airfoil model, Fig. 4.

Two-Dimensional Evaluation of Dual-Radius CCW Airfoil

Initially, force and moment coefficients plus static pressure distributions were recorded for this baseline CCW/Supercritical airfoil with the Krueger leading-edge flap deflected 60 deg and the 10.9% chord dual-radius flap deflected 90 deg. Figure 5 shows an aft view of the deflected flap with blowing applied. A cotton tuft reveals the large jet turning angle at the flap trailing edge. Figures 6 and 7 show reduced and corrected[12] balance data for this two-dimensional airfoil (labeled "MTF12") in comparison to data previously recorded for the semispan version of the same configuration (labeled "T158"), all taken at a geometric incidence of $\alpha = 0$ deg. The production data was taken at a dynamic pressure of 10 psf to limit larger aerodynamic loads and possible grounding of the balance, and is thus somewhat conservative, not taking advantage of the favorable Reynolds number effect shown. Also evaluated were the effects of variation in blowing slot height h (also discussed in Refs. 2, 4, 5, 7, and 8). In Fig. 6, two-dimensional lift values 26 to 43% greater than those of the semispan model are seen, primarily due to the elimination of the strong tip vorticity and improved test setup for the present two-dimensional data. Corresponding to this elimination of the induced finite-span effects are the 21–68% lower values of measured two-dimensional drag coefficient seen in

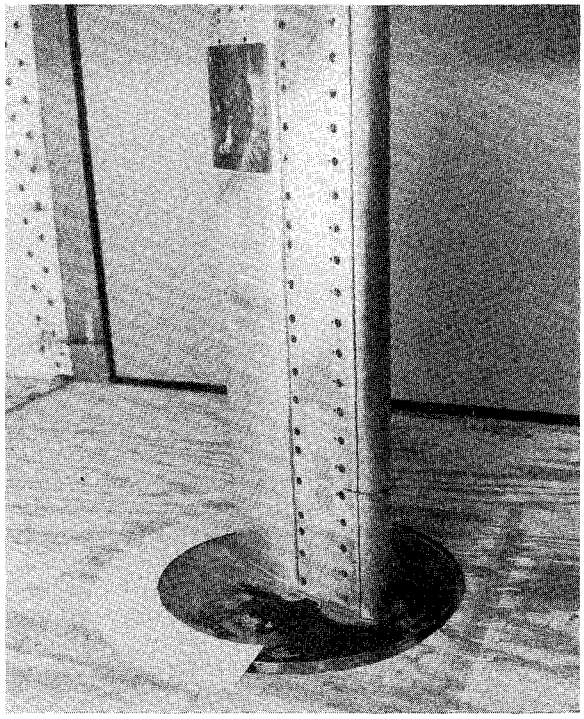

Fig. 5 Aft view of CCW dual-radius two-dimensional airfoil showing jet turning and attachment to 90-deg CCW flap.

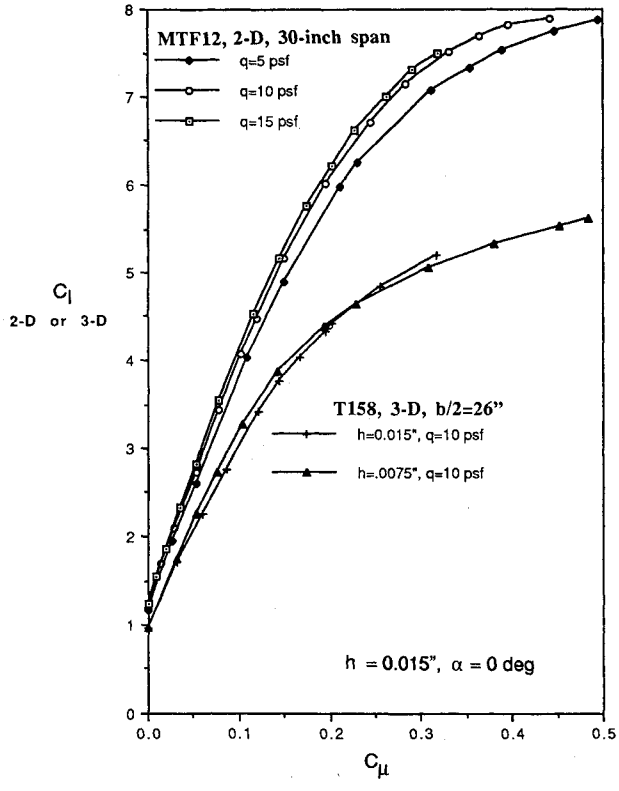

Fig. 6 Comparison of two-dimensional airfoil and three-dimensional semispan lift results for the dual-radius CCW model at α = 0 deg (60-deg Krueger and 90-deg CCW flap deflections).

Fig. 7. These data emphasize the large difference between two- and three-dimensional data, and stress the importance of adequate two-dimensional test techniques.[12] Also of interest in Fig. 7 is the initial reduction of the two-dimensional drag as the blowing reduces separation on the highly deflected flap.

The above results represent a significant increase in lift-augmenting capability compared to previous CCW configu-

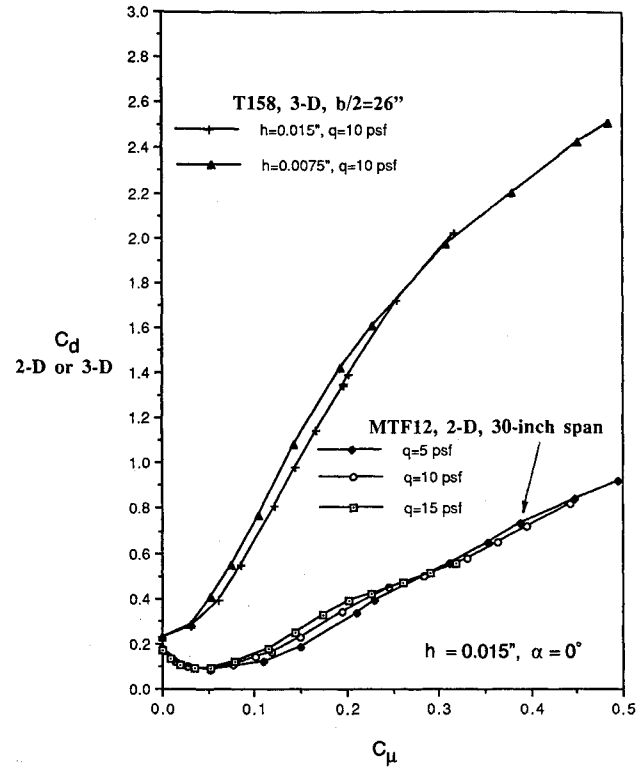

Fig. 7 Comparison of two-dimensional airfoil and three-dimensional semispan drag results for the dual-radius CCW model at α = 0 deg (60-deg Krueger and 90-deg CCW flap deflections).

rations. In Fig. 1, the lift of this dual-radius CCW airfoil is compared at α = 0 deg to the state-of-the-art high-lift airfoils and to earlier CCW configurations. Lift improvement of up to 35% over previous two-dimensional CCW airfoils is due partly to the increased unblown camber of the short-chord flap, and partly to the increased lift-augmentation capabilities provided by the greater CCW turning-surface radius on the flap. Lift values approaching 8.0 at 0-deg incidence and relatively low momentum coefficient represent a factor of from 1.8 to 4 increase over the zero-incidence lift values for the various mechanical flaps surveyed in Fig. 1. Furthermore, when these are added to a lift curve slope of 0.1/deg (or more, to be shown below), an effective leading-edge device should be able to yield $C_{l\,max}$ values in the 9 or greater range. It is significant to note that these two-dimensional pneumatic high-lift values recorded on the present CCW model are the highest ever recorded at these lower blowing rates by the first author in his 20+ yr of experience in test and evaluation of blown airfoils and wings.

This lift-generating ability is further emphasized by the static pressure distributions shown in Fig. 8, where very high trailing-edge suction peaks result in flow entrainment and circulation enhancement. However, even at α = 0 deg, these distributions reveal the beginning of leading-edge separation on the Krueger flap at higher blowing, amplifying the need for a more effective pneumatic nonmechanical leading edge. Figure 9 shows variations in static pressure distributions as angle of attack is increased at a constant blowing value, and reveals the same type of LE separation.

To provide a baseline reference for the performance increase due to blowing on the dual-radius CCW, the flap was retracted to the cruise position (trailing edge located on the chord line), and the Krueger leading edge was removed. Figure 10 denotes the large aerodynamic differences between the high-lift and cruise configurations at 3 blowing rates: 0.0, 0.15, and 0.28. It also shows the increase in stall angle provided by the mechanical LE device. The augmentation effects of large jet turning, flow entrainment, and supercirculation on the overall airfoil characteristics are obvious. The dual-radius CCW

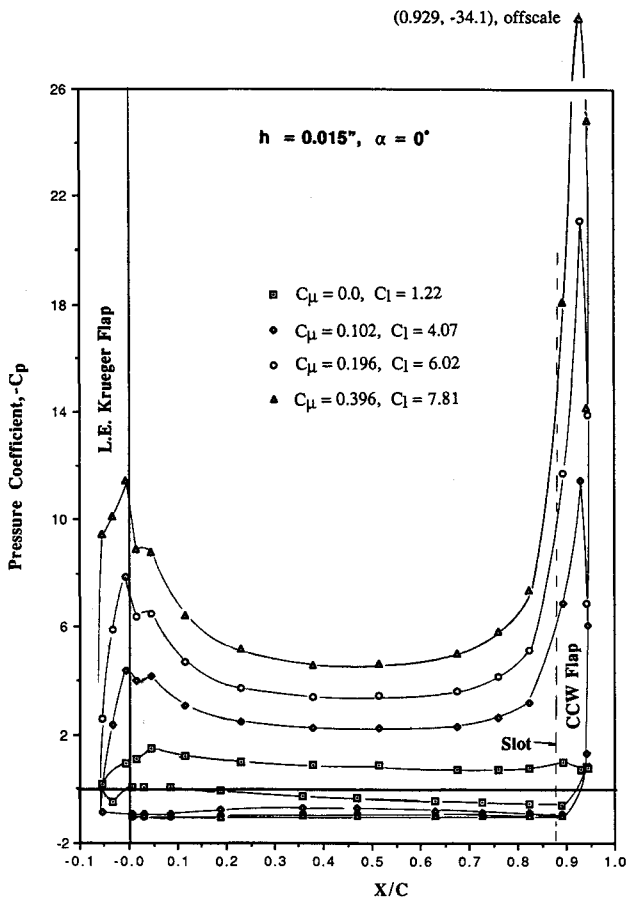

Fig. 8 Chordwise static pressure distributions for two-dimensional dual-radius CCW airfoil at $\alpha = 0$ deg and $q = 10$ psf (60-deg Krueger and 90-deg CCW flap deflections).

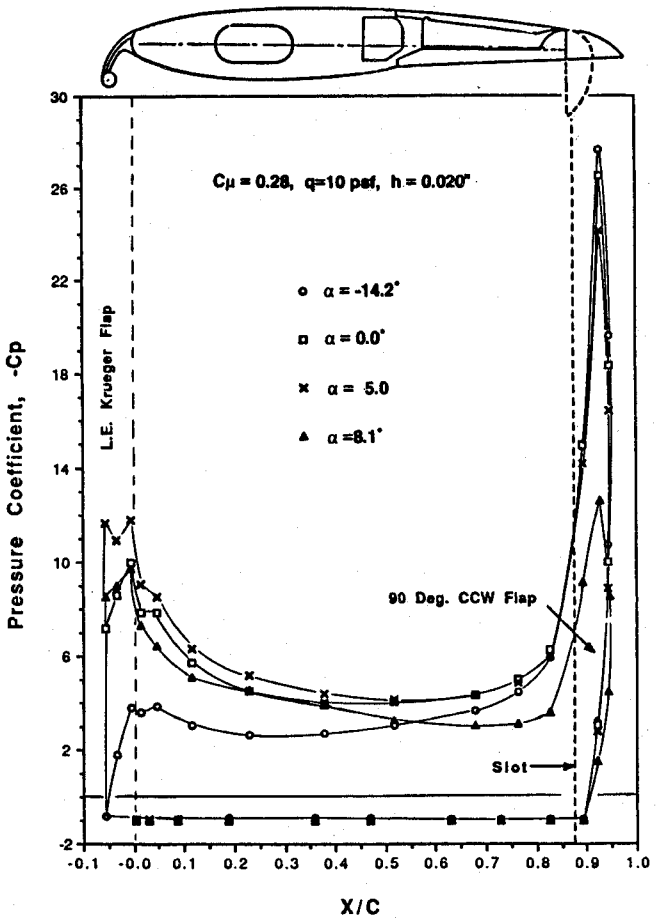

Fig. 9 Chordwise static pressure distributions for the dual-radius CCW airfoil, (60-deg Krueger and 90-deg CCW flap).

configuration with large deflections of the short-chord flap thus demonstrates very effective lift-generating capability as long as adequate leading-edge separation prevention is provided.

Pneumatic Leading-Edge Devices

Leading-Edge Effectiveness

Development of pneumatic or mechanical flap systems brings with it the essential requirement for effective leading-edge (LE) devices to prevent flow separation at large values of supercirculation, whether these values be produced by high incidence, mechanical camber, or pneumatic flow entrainment.[15] The current two-dimensional airfoil employs a Krueger leading-edge flap deflected 60 deg (Fig. 3), a state-of-the-art device commonly used on commercial and military transport aircraft. Its effectiveness in increasing stall angles and maximum lift coefficients is emphasized in Fig. 11, when compared to the same 90-deg-flap CCW airfoil with the Krueger flap retracted. The stall angle is increased by 6–7 deg for the unblown flap, and by 15 deg or more as flap C_μ is increased. However, the Krueger's effectiveness at high supercirculation values is still limited, as stall occurs at less than $\alpha = 5$ deg at higher C_μ values. Also, at lower lift and incidence, the 60-deg Krueger flap stalled on its lower surface. These results clearly emphasize the need for a more effective leading-edge device. To develop an appropriate blown leading edge, CFD codes (to be discussed below) were used to analyze suction peaks experienced in the leading-edge pressure distributions. Over an anticipated range of lift, blowing, and incidence, the blowing slot needed to be located slightly ahead of the adverse pressure gradient so that it could entrain the flowfield and delay separation.

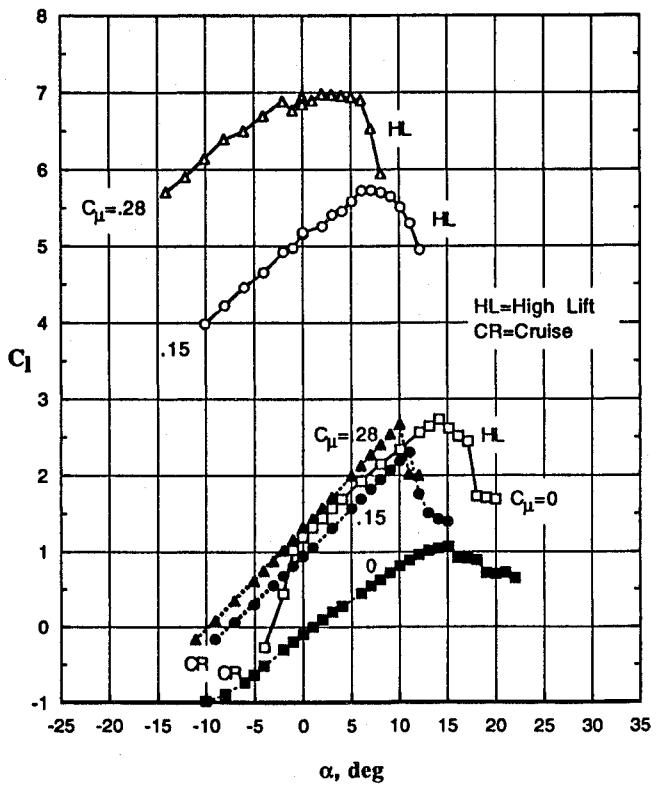

Fig. 10 Comparison of high-lift (60-deg Krueger and 90-deg CCW) and cruise CCW airfoil configurations.

Investigation of Dual-Slot CCW Airfoil

A preliminary dual-slot CCW airfoil was assembled by combining a CFD-designed blown leading-edge contour with the baseline CCW dual-radius aft flap assembly of Fig. 3. Figure 12 shows this model and the associated static pressure tap locations. Several slot height values and internal plenums were tested. The ability of this pneumatic LE to deter flow separation is shown in Fig. 13. Here, for two values of blowing on the CCW flap, variation in leading-edge blowing is shown. For reference, the clean (Krueger-retracted K_0) configuration is also shown. Compared to the clean leading edge, an increase of 2–4 deg in stall angle was produced by the aft-facing LE slot with blowing off. A significant gain in stall angle (10–13 deg) was produced by applying $C_{\mu LE} = 0.10$. Additional LE blowing above this amount was somewhat less productive. It was also found that increased LE blowing momentum was recovered as thrust (negative drag).

Figure 14 compares the effectiveness of LE blowing ($C_{\mu LE} = 0.18$) to the 60-deg Krueger flap. For zero and low CCW flap blowing, LE blowing has several strong effects. It extends the stall angle 6–7 deg beyond the Krueger value, eliminates the lower surface stall on the Krueger, and adds a lift increment while preserving the lift-curve slope. At higher CCW flap blowing, the pneumatic LE continues to yield higher stall angles than the Krueger, and makes the stall less severe by forcing aft rather than leading-edge separation. For all values of trailing-edge blowing, the Krueger LE is surpassed by the blown LE in both $C_{L\max}$ and stall angle achieved. This improved LE performance was produced by a redesigned internal plenum yielding more uniform spanwise flow than from the original slot configuration. The known improvement[7,8,10] due to smaller slot height has been incorporated into this configuration. The uppermost curve of Fig. 14 shows the improvement in $C_{L\max}$ and stall angle available if increased LE and TE blowing are available. The effectiveness of the pneumatic leading-edge has thus been verified as a means to extend the stall angle, increase usable lift and "soften" the stall.

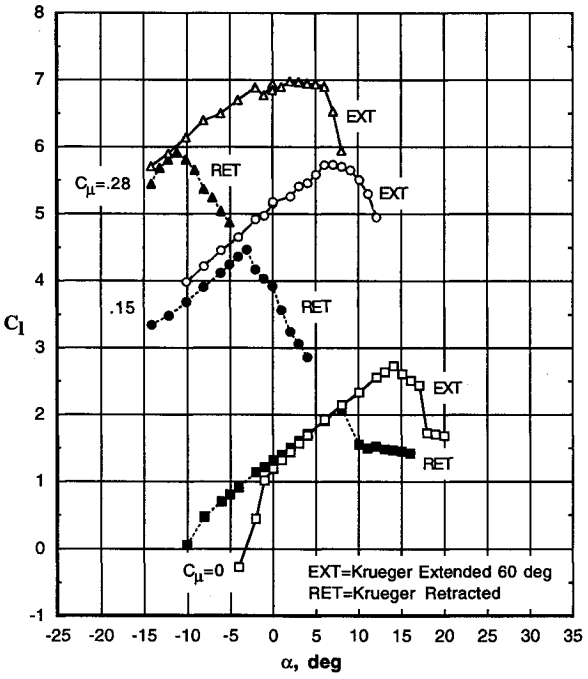

Fig. 11 Effect of adding Krueger leading-edge device to dual-radius airfoil with 90-deg CCW flap deflection.

This was further confirmed by the static pressure distributions shown in Figs. 9 and 15. Note the significant differences in the vicinity of the leading edge. The high LE jet velocity yields high negative pressure coefficients (Fig. 15) compared to those of the Krueger flap (Fig. 9). The concept of a blown leading edge offers significant potential here. The mechanical retraction/deployment components are eliminated. When blowing is terminated, the device becomes transparent. It does not experience lower surface stall at low incidence, and it surpasses the Krueger flap in keeping leading-edge flow attached at high incidence and lift. In addition, if applied in conjunction with a blown trailing-edge flap, its blowing schedule can be coupled directly to that of the flap, so that increased leading-edge protection occurs with increased supercirculation. The experimental evaluations thus confirmed these high-lift capabilities of CCW airfoils, and that this lift could be augmented by variations in angle of attack, blowing coefficients, flap deflections, and/or blowing slot heights.

Analytical Development of Circulation Control Airfoils

Design of the improved CCW airfoils was aided by the use of in-house viscous-flow CFD codes. The complex flowfields about circulation control (CC) airfoils with multiple jets are governed by highly interactive viscous and inviscid flow regions. Previous lower-order methods for computational analysis of single-slot CC airfoils[16–19] have consisted of weakly coupled viscid-inviscid methods. While good results have been obtained via these methods, a comprehensive analysis of the force characteristics of multiple slot/flap airfoils requires an analysis method that accounts for the strongly coupled nature of the different flow regimes.

Therefore, a two-dimensional Navier-Stokes solver with imbedded jet characteristics is appropriate to produce simulations for both blown and nonblown airfoils, thus providing continuity of force predictions. Several of these solvers[20,21]

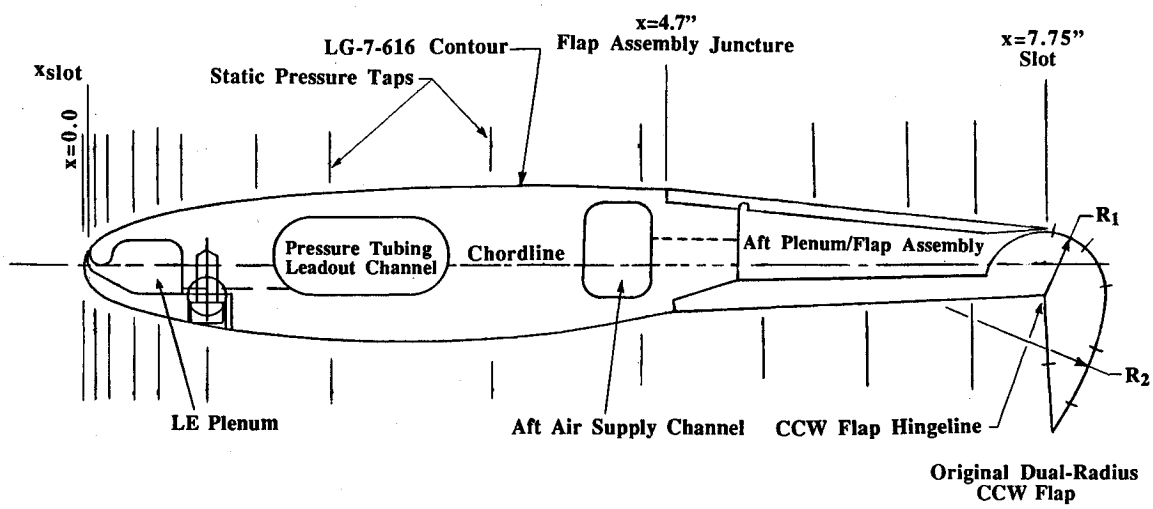

Fig. 12 Dual-slot, dual-radius CCW two-dimensional airfoil model.

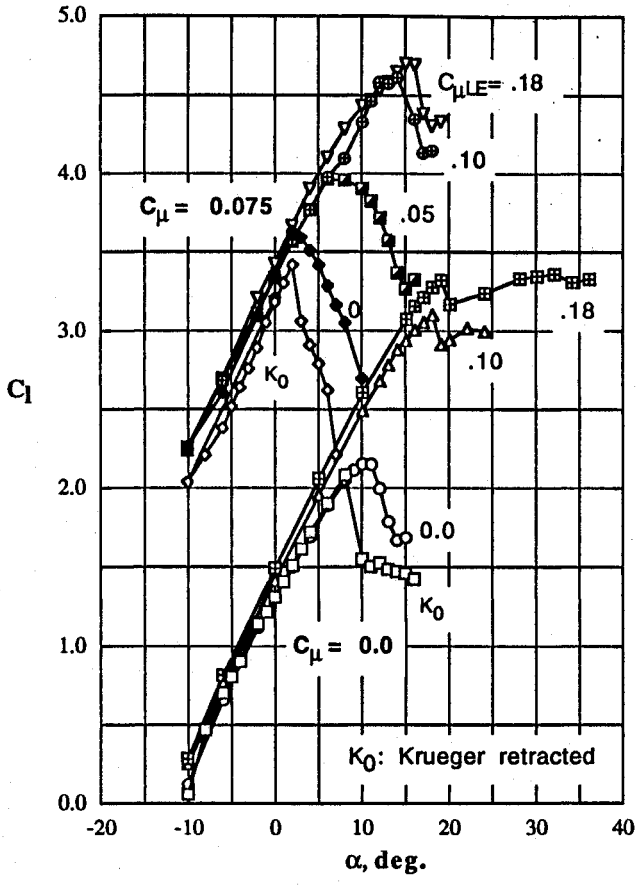

Fig. 13 Effectiveness of LE blowing in delaying stall onset.

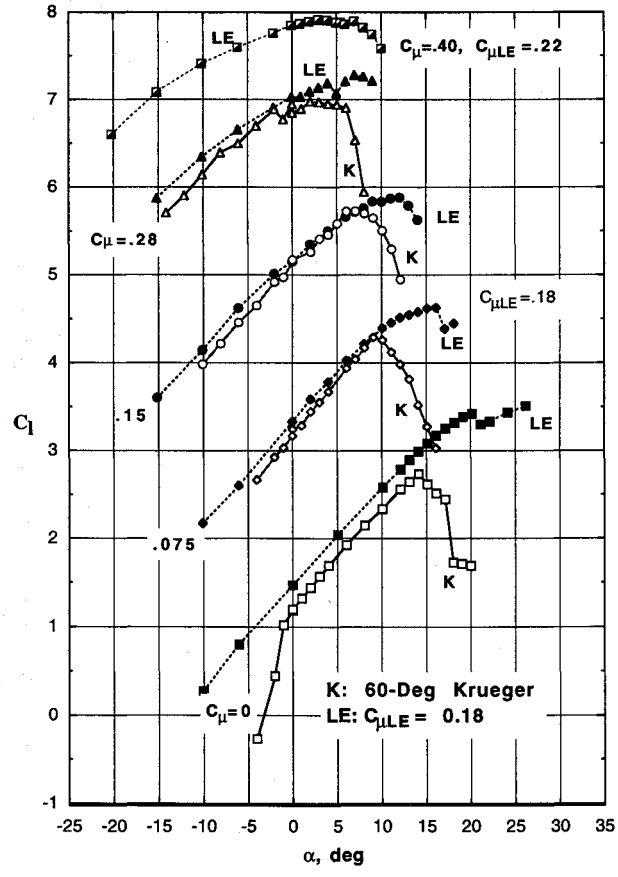

Fig. 14 LE blowing effectiveness compared to Krueger flap, $C_{\mu LE}$ = 0.18.

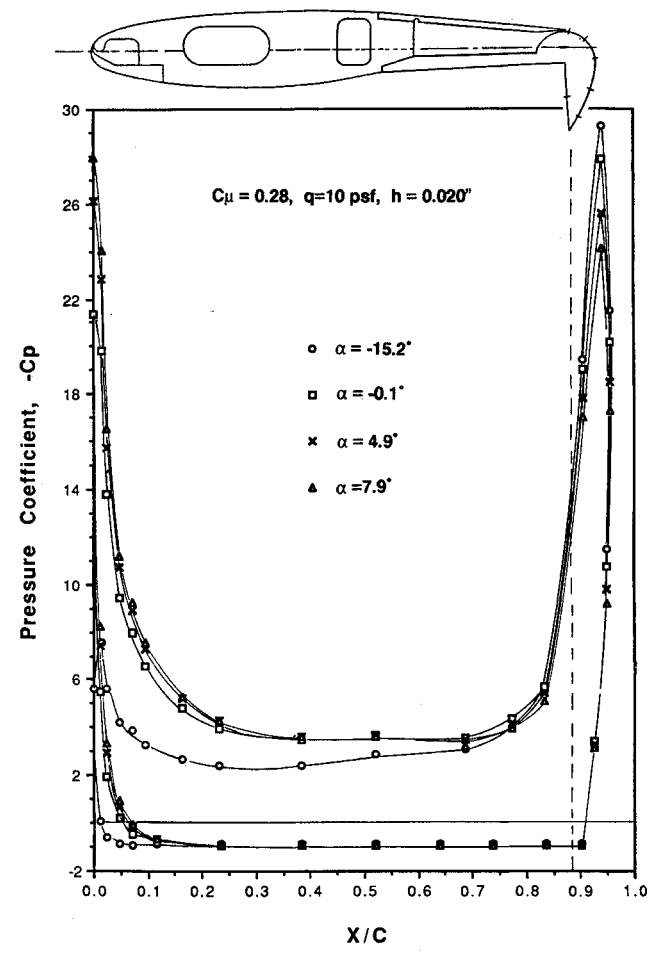

Fig. 15 Chordwise static pressure distributions for dual-slot, dual-radius CCW airfoil with $C_{\mu LE}$ = 0.10.

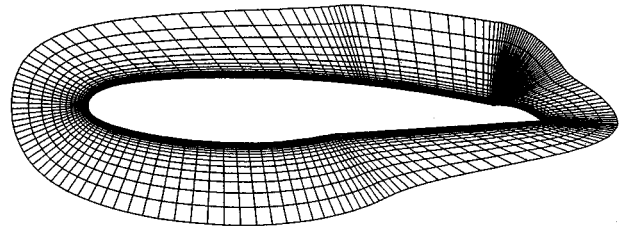

Fig. 16 Closeup of grid near the original dual-radius CCW airfoil at cruise condition.

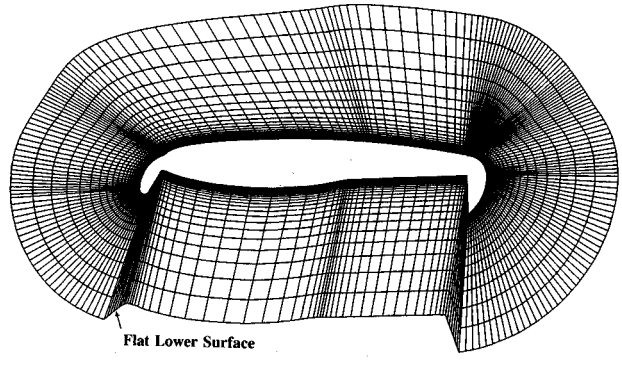

Fig. 17 Closeup of grid near the dual-radius CCW airfoil in the high-lift configuration.

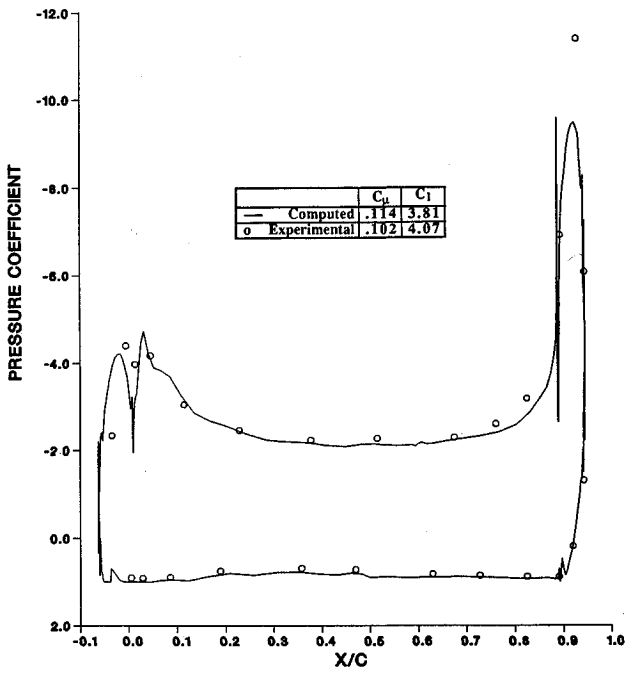

Fig. 18 Pressure distributions on dual-radius CCW airfoil with aft flap at 90 deg, Krueger flap at 60 deg, α = 0 deg, and C_μ = 0.10.

are currently available, including one developed by Georgia Tech[22] and Lockheed known as GT2DNSCC (Georgia Tech 2-D Navier-Stokes Circulation Control). The solver is based on a conventional two-dimensional Navier-Stokes method developed at Georgia Tech that has been applied and validated for a number of steady and unsteady applications[23,24] with conventional airfoil geometries. This Georgia Tech methodology is considered to be an industry standard in two-dimensional Navier-Stokes solvers, and is currently in use at several U.S. companies.[25]

The solver utilized in this project is based on GT2DNSCC, where the unsteady two-dimensional Reynolds-averaged, compressible Navier-Stokes equations are solved in a body fitted coordinate system using an alternating direction implicit (ADI) procedure. An in-depth discussion of the numerical details of the solver is given in Ref. 26. Two examples of the user-defined grid generation input are shown in Figs. 16 and 17, the first representing the clean cruise airfoil, and the second representing the CCW high-lift configuration, with the leading edge deployed.

The CFD simulations were first applied to locate the correct placement for the leading-edge slot. Positive angle-of-attack sweeps were performed analytically on the candidate airfoils at a Mach number of 0.1. By determining the chordwise location of the suction peaks at various angles of attack, the jet slot was located forward of the adverse pressure gradient to boost that suction peak and to avoid premature separation at higher angles of attack. The leading-edge design shown in Fig. 12 resulted from this analysis.

The CFD codes were also used to predict blown high-lift performance. Figure 18 shows a typical computed blown pressure distribution in comparison to measured data from the tunnel test. Agreement is quite good for this highly viscous flow case, with only small discrepancies noted due to slight variations in theoretical vs actual model geometry, actual blowing slot height when pressurized, and actual angle of attack.

One of the primary tasks of this study was to investigate the cruise performance of CCW airfoils since no compressible flow testing had been conducted. Cruise performance for the conventional and circulation control airfoils with flaps retracted was predicted for Mach numbers from 0.1 to 0.8, and drag polars were generated up through compressible speeds.

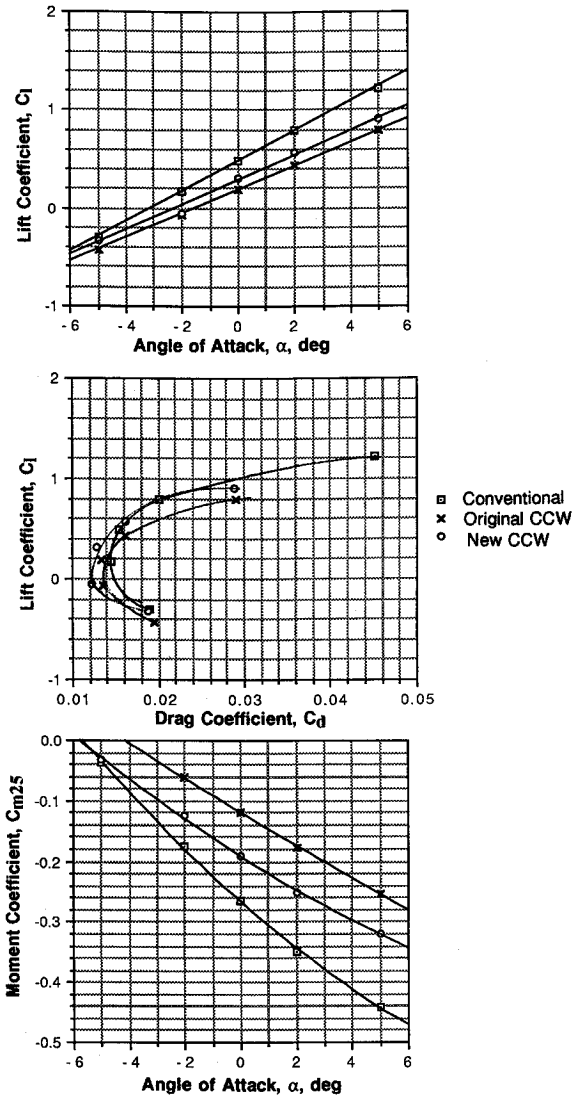

Fig. 19 Computed cruise performance characteristics at Mach-0.6 for conventional supercritical, original CCW, and modified CCW airfoils (no blowing).

A typical set of performance curves for unblown cruise configurations is shown for a Mach number of 0.6 in Fig. 19. The conventional airfoil (the upper configuration in Fig. 3) provides the best overall performance due to the thinner cusped trailing edge. The original CCW airfoil, which was based on previous CC airfoils and is shown in Fig. 16, had the poorest higher-speed performance. The new CCW airfoil, which incorporated many of the conventional airfoil shape features ahead of the slot and modified CC features downstream, showed a great improvement over the original CCW airfoil's characteristics. As angle of attack increases, the cruise performance of the CCW airfoils diminishes with respect to that of the conventional supercritical airfoil with aft camber. This is due to the effect of the discontinuity formed by the leading-edge blowing slot on the CC airfoils. It implies that the leading-edge slot should be as thin as possible. In actual use, it could be designed as a flexible lip, opened only when pressurized for low-speed, high-lift operation. At 4-deg angle of attack and lower, especially at lower Mach numbers, the cruise performance of the new CCW airfoil approaches or is equivalent to the original supercritical airfoil's performance.

Further details of this CFD analysis as well as additional details on test technique and results can be found in Ref. 27.

Conclusions

The above experimental and analytical results confirm the high-lift potential (C_l of 8 at α = 0 deg) of CCW advanced

airfoils aided by leading-edge blowing. Control of lift, drag, and pitching moments on these airfoils was provided by variations in blowing rate, angle of attack, LE or TE flap deflections, and blowing slot height. Extension of the computational analyses to cruise conditions indicates that new CCW airfoil shapes maintain good cruise characteristics at nonblown conditions, unlike previous larger TE radius blown airfoil geometries.

These results offer the potential for reduced complexity and lower terminal-area noise levels for subsonic transport aircraft equipped with CCW high-lift systems, and indicate similar payoffs for higher-speed transports. The results strongly suggest the potential of practical CCW transport configurations to provide the following capabilities, and it is thus recommended that further development be pursued:

1) CCW performance will greatly reduce takeoff and landing speeds, yielding reduced runway lengths and increased safety of flight in terminal areas.

2) Steep climbout and approach flight paths due to STOL capability can yield reduced noise exposure to surrounding communities.

3) Greatly increased liftoff gross weight and landing weight provided by smaller wing area will allow transport wings that are more optimized for cruise and greater fuel efficiency.

4) Pneumatic CCW configurations will greatly reduce high-lift system complexity, as will the combination of high-lift, roll-control, and direct-lift-control surfaces into a single multipurpose pneumatic wing/control surface.

Part II of this article discusses the application of circulation control technology to a typical subsonic transport aircraft, and further emphasizes these potential payoffs.

Acknowledgments

This project was sponsored by NASA Langley Research Center under Contract NAS1-19061. Work currently under way and just briefly reported on here is being funded under Grant NAG1-1517. The NASA Technical Monitor was Edgar G. Waggoner, Head, Subsonic Aerodynamics Branch, to whom the authors would like to express their appreciation for his support and encouragement.

References

[1]Englar, R. J., and Applegate, C. A., "Circulation Control-A Bibliography of DTNSRDC Research and Selected Outside References (Jan. 1969 to Dec. 1983)," David Taylor Naval Ship R&D Center Rept. (DTNSRDC) 84/052, Bethesda, MD, Sept. 1984.

[2]Englar, R. J., "Experimental Investigation of the High Velocity Coanda Wall Jet Applied to Bluff Trailing Edge Circulation Control Airfoils," Naval Ship R&D Center (NSRDC) Rept. 4708, Aero Rept. 1213, AD-A-019-417, Bethesda, MD, Sept. 1975.

[3]Jones, D. G., "Measurements of Wall Jet Development on a Circulation Control Aerofoil," Ph.D. Dissertation, Mechanical Engineering Dept., Univ. of California, Davis, Davis, CA, Jan. 1971.

[4]Englar, R. J., "Two-Dimensional Subsonic Wind Tunnel Tests of Two 15-Percent-Thick Circulation Control Airfoils," Naval Ship R&D Center, NSRDC TN AL-211, Bethesda, MD, Aug. 1971.

[5]Englar, R. J., "Development of the A-6/Circulation Control Wing Flight Demonstrator Configuration," David Taylor Naval Ship R&D Center, DTNSRDC Rept. ASED-79/01, Bethesda, MD, Jan. 1979.

[6]Williams, R. M., and Howe, H. J., "Two-Dimensional Subsonic Wind Tunnel Tests of a 20-Percent Thick, 5-Percent Cambered Circulation Control Airfoil," Naval Ship R&D Center, NSRDC TN AL-176, Bethesda, MD, Aug. 1970.

[7]Englar, R. J., "Low-Speed Aerodynamic Characteristics of a Small Fixed-Trailing Edge-Circulation Control Wing Configuration Fitted to a Supercritical Airfoil," David Taylor Naval Ship R&D Center, DTNSRDC Rept. ASED-81/08, Bethesda, MD, March 1981.

[8]Englar, R. J., and Huson, C. G., "Development of Advanced Circulation Control Wing High-Lift Airfoils," AIAA Paper 83-1847, July 1983; see also *Journal of Aircraft*, Vol. 21, No. 7, 1984, pp. 476–483.

[9]Wilson, M. B., and Von Kerczek, C., "An Inventory of Some Force Producers for Use in Marine Vehicle Control," David Taylor Naval Ship R&D Center, DTNSRDC-79/097, Bethesda, MD, Nov. 1979.

[10]Englar, R. J., Hemmerly, R. A., Moore, W. H., Seredinsky, V., Valckenaere, W. G., and Jackson, J. A., "Design of the Circulation Control Wing STOL Demonstrator Aircraft," AIAA Paper 79-1842, Aug. 1979.

[11]Pugliese, A. J., and Englar, R. J., "Flight Testing the Circulation Control Wing," AIAA Paper 79-171, Aug. 1979.

[12]Englar, R. J., and Williams, R. M., "Test Techniques for High Lift Two-Dimensional Airfoils with Boundary Layer and Circulation Control for Application to Rotary Wing Aircraft," *Canadian Aeronautics and Space Journal*, Vol. 19, No. 3, 1973, pp. 93–103; see also Naval Ship R&D Center, NSRDC Rept. 4645, Bethesda, MD, July 1975.

[13]Englar, R. J., Schuster, D. M., and Ford, D. A., "Experimental Evaluations of the Aerodynamics of Unlimited Racing Hydroplanes Operating In and Out of Ground Effect," Society of Automotive Engineers Paper 901869, Oct. 1990; see also *SAE 1990 Transactions, Journal of Aerospace*, Sec. 1, Vol. 99, Pt. 2, 1991, pp. 1615–1624.

[14]Englar, R. J., "The Application of Circulation Control Pneumatic Technology to Powered-Lift STOL Aircraft," Society of Automotive Engineers Paper 872335, Dec. 1987; see also *Proceedings of the International Powered Lift Conference* (Santa Clara, CA), 1988, pp. 357–369 (SAE P-203).

[15]Kohlman, D. L., *Introduction to V/STOL Airplanes*, Iowa State Univ. Press, Ames, IA, 1981, pp. 123–165.

[16]Gibbs, E. H., and Ness, N., "Analysis of Circulation Controlled Airfoils," West Virginia Univ. Dept. of Aerospace Engineering, Rept. TR-43, Morgantown, WV, June 1975.

[17]Dvorak, F. A., and Kind, R. J., "Analysis Method for Viscous Flow over Circulation-Controlled Airfoils," *Journal of Aircraft*, Vol. 16, No. 1, 1979, pp. 23–28.

[18]Dvorak, F. A., and Choi, D. H., "Analysis of Circulation Controlled Airfoils in Transonic Flow," *Journal of Aircraft*, Vol. 20, No. 4, 1983, pp. 331–337.

[19]Dash, S. M., and Wolf, D. E., "Viscous/Inviscid Analysis of Curved Wall Jets: Part 1-Inviscid Shock Capturing Model (SCIPWJET)," SAI/PR TR-5, Princeton, NJ, Sept. 1982.

[20]Berman, H. A., "A Navier-Stokes Investigation of a Circulation Control Airfoil," AIAA Paper 85-0300, Jan. 1985.

[21]Pulliam, T. H., Jesperson, D. C., and Barth, T. J., "Navier-Stokes Computations for Circulation Controlled Airfoils," AIAA Paper 85-1587, July 1985.

[22]Shrewsbury, G. D., "Analysis of Circulation Control Airfoils Using an Implicit Navier-Stokes Solver," AIAA Paper 85-0171, Jan. 1985.

[23]Wu, J.-C., "A Study of Unsteady Turbulent Flow Past Airfoils," Ph.D. Dissertation, Georgia Inst. of Technology, Atlanta, GA, June 1988.

[24]Sankar, N. L., and Tang, W., "Numerical Solution of Unsteady Viscous Flow Past Rotor Sections," AIAA Paper 85-0129, Jan. 1985.

[25]Smith, M. J., and Hassan, A. H., "Improvement to Interactive Two Dimensional Rotor Section Design," American Helicopter Society Vertical Lift Aircraft Design Conf., San Francisco, CA, Jan. 1990.

[26]Shrewsbury, G. D., "Dynamic Stall of Circulation Control Airfoils," Ph.D. Dissertation, Georgia Inst. of Technology, Atlanta, GA, Nov. 1990.

[27]Englar, R. J., Smith, M. J., Kelley, S. M., and Rover, R. C., III, "Development of Circulation Control Technology for Application to Quiet Advanced Subsonic Transport Aircraft," Georgia Tech. Research Inst. Rept. A-8612-006, Dec. 1991.